RECENT PROGRESS IN THE DEVELOPMENT OF THE OPTIMAL SPECTRAL SAMPLING (OSS) METHOD

3.5 Jean-Luc Moncet*, Gennadi Uymin and Karen Cady-Pereira
Atmospheric and Environmental Research, Inc., Lexington, MA, USA

1. INTRODUCTION

Radiative transfer models are an integral part of remote sensing and radiance assimilation systems and are also used to support instrument design trades and performance analysis. To extend beyond ongoing research efforts and be effective in the operational environment a radiative transfer model must have sufficient radiometric accuracy for the problem at hand while also possessing a high degree of computational efficiency. However, computational speed often comes at the expense of overall radiometric accuracy or limitations in the ability to adapt the model to changes in sensor or mission parameters. A further limitation of models designed for operational use is that they tend to be based on the parameterization of atmospheric optical depth. In this case the radiative transfer no longer obeys Beer's law and is not amenable to multiple scattering atmospheres. Also, for many types of parameterizations it is inefficient to calculate the radiance Jacobians (the change in radiance with respect to a geophysical quantity) necessary for retrieval calculations, and the overall accuracy depends strongly on the choice of predictors.

In order to address these concerns we have set some criteria that must be met for the development of a robust, computationally efficient model for generic remote sensing applications. Most importantly, the model must be applicable to a wide range of remote sensing problems, with only minor configuration changes: down-looking (satellite sensors), up-looking (ground-based sensors), aircraft or balloon (variable viewing and altitude ranges), limb or line-of-sight measurements, and the inverse adjoint for radiance assimilation algorithms. In order to make the process of multi-sensor data fusion all the more tractable, the ideal model must have consistent physics throughout all spectral ranges, from the microwave through the ultraviolet, and be applicable to both narrow-band and wide-band applications. It will also work equally well in scattering and non-scattering atmospheres and be easy to couple with multiple-scattering and/or atmospheric polarization models. Both accuracy and execution speed are important parameters and the ideal model would allow a trade-off depending on the specifics of the problem. Such a trade-off should allow for both highly accurate calculations of total radiance as well as high accuracy for each of the individual layers in the calculation. (Thus the model would be suitable for both "atmospheric correction" and radiance inversion problems). Finally, the algorithm should be capable of calculating the radiance Jacobians (derivative of radiance with respect to geophysical parameters) necessary to perform the radiance inversion, and to consider any number of gases as having fixed or variable (retrievable) amounts. The Optimal Spectral Sampling (OSS) approach meets these criteria and directly addresses the need for highly accurate real-time monochromatic radiative transfer calculations (including the Jacobians) for any class of multispectral, hyperspectral, or ultraspectral sensor.

The Optimal Spectral Sampling (OSS) method (e.g. Moncet *et al.*, 2004) is a fast and accurate transmittance parameterization technique. The OSS method offers a simple and practical solution to the problem of extending the Exponential Sum Fitting of Transmittances (ESFT) (Wiscombe, 1977) and *k*-distribution techniques (e.g. Goody *et al*, 1989) to vertically inhomogeneous atmospheres with overlapping absorbing species. The multi-dimensional search for absorption coefficients (*k*'s) in a multi-layered atmosphere attempted by several authors (e.g. Armbruster and Fischer, 1996) is greatly simplified by operating in the one-dimensional frequency domain. In the OSS concept (US Patent #6,584,405), the parameterization process reduces to searching for a set of wavenumbers (nodes) and associated weights such that spectrally integrated radiances (or transmittances) are well approximated by a linear combination of monochromatic radiances computed at the selected nodes,

$$\bar{R} = \int_{\Delta\nu} \phi(\nu) R(\nu) d\nu = \sum_i w_i R(\nu_i) \qquad (1)$$

Like current transmittance parameterizations employed operationally in retrieval and radiance assimilation systems, the OSS method requires a globally representative set of atmospheric profiles for training. As an example of this fitting, consider the spectrum measured by a nadir-viewing spacecraft sensor (shown in Figure 1). The left panels of the figure show the spectrum as a function of total optical depth (top line) and decomposed by different molecular species at different levels of the atmosphere. The vertical lines give an example of the node locations selected by OSS for a channel encompassing this spectral range. The top panel is for a radiometric brightness temperature threshold of 0.05K, while the bottom panel is for 0.01K. The right panels show the overall top-of- atmosphere

* *Corresponding author address:* Jean-Luc Moncet, AER, Inc, 131 Hartwell Ave, Lexington, MA 02421
Tel: 781-761-2267; e-mail: jmoncet@aer.com

brightness temperature for a calculation in this spectral region. The upper panels are for a lower radiometric threshold and thus require fewer points to minimize the error with the monochromatic calculation.

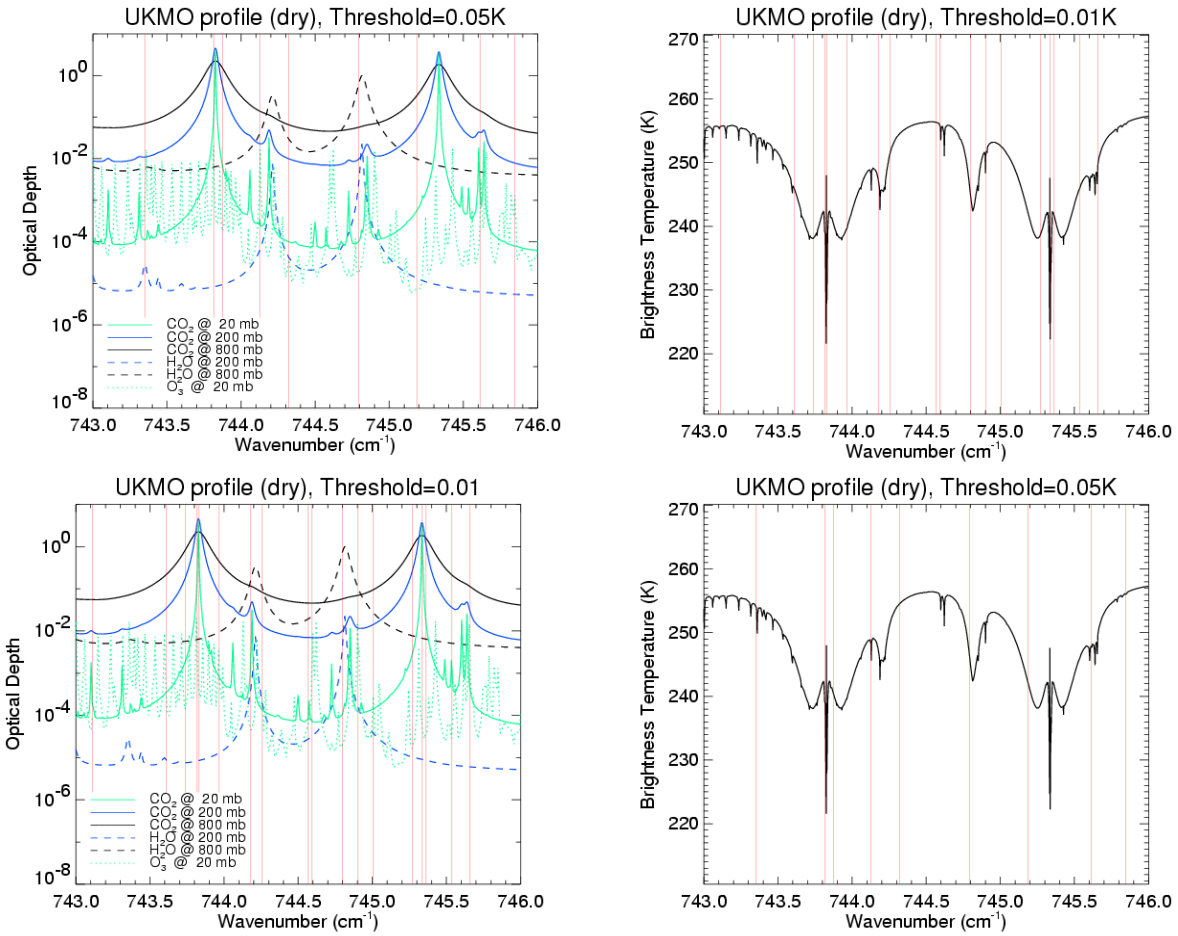

Figure 1: Example of OSS node selection for a region of the mid-infrared spectrum. The left panels indicate the selected nodes relative to the optical depth spectrum, while the panels on the right give selected nodes as a function of total (top-of-atmosphere) brightness temperature. The thin vertical lines represent the locations of selected nodes.

Initially, we have concentrated on trading and optimizing techniques for selecting the nodes and weights for a single channel, in non-scattering atmospheres (e.g. Moncet and Uymin, 2003). The microwave and infrared models produced in this first phase of development already offer significant speed and accuracy advantages over current operational radiative transfer (RT) models (Weng *et al.*, 2005). OSS models are currently used in the NPOESS/CrIS and CMIS EDR algorithms (Moncet *et al.*, 2004, 2001) and have been integrated in the Joint Center for Satellite Data Assimilation (JCSDA) Community RT Model (CRTM) model (van Delst *et al.*, 2005.), a joint NOAA/AER effort. These models are currently being considered for operational use in the National Center for Environmental Prediction (NCEP) assimilation process. In addition, a version of OSS is currently under development for direct inclusion into the MODTRAN model, as an alternative to current band models. As part of transitioning the OSS technology to NCEP the OPTRAN and OSS models have been extensively compared at NOAA. While the OSS model is more accurate than OPTRAN for all the operational instruments considered (e.g. Figure 2) , its speed is about 8 times faster for the high spectral resolution AIRS instrument (e.g. Weng *et al.*, 2005). Recent research has focused on extending the current training to scattering atmospheres and on training models for high spectral resolution instruments by considering all the channels simultaneously (generalized training). Some key results of this research are presented below.

2. GENERALIZED OSS TRAINING

In the first phase of development of OSS we have focused on single channel (localized) training. This form of training leads to an optimal (in terms of the number of nodes used to achieve a prescribed accuracy) node selection for the individual channels.

When the RT model operates on the same set of channels, it is advantageous to consider all the channels at once in the training. In the generalized "multi-channel" training one exploits the correlations in the spectrum in an attempt to maximize the number of nodes that are common to several channels and thereby reduce the total number of nodes used to describe the channel set.

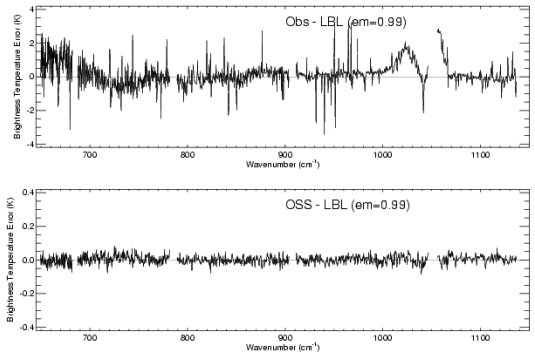

Figure 2: Example of AIRS model validation. The top plot shows the difference between actual observation and line-by-line calculations for a selected RAOB at ARM Tropical Western Pacific site. The bottom plot shows difference between and OSS and LBLRTM line-by-line calculations (note that the scale has been blown up by a factor 10)

Figure 3 shows the correlation matrix for the 645-2690 cm^{-1} domain (AIRS instrument bandwidth).

Two methods are currently being used for the multi-channel training. The first method is a direct extension of the single channel selection approach in which one keeps on adding nodes until the *rms* difference between exact and approximate radiances fall below a given threshold for all individual channels within a set of *N* (not necessarily contiguous) channels. The second method is a clustering type technique. Starting from the complete set of candidate nodes for the group of channels, this method successively reduces the number of nodes by merging together nodes containing highly correlated information. The correlation radius is a function of the desired accuracy. The latter approach is faster than the first method and may handle much wider spectral domains. However more work is required to make its selection optimal.

Examples of application of generalized clear-sky training are shown in Table 1. For $1cm^{-1}$ wide boxcar functions, the gains in speed (and memory requirements) over the single channel approach are as large as 10-20 (for AIRS our current gain estimate is ~7, which brings the average number of nodes per channel from ~2 to ~0.3). In cloudy skies, spectral variations in cloud/aerosols optical properties tend to reduce the large-scale correlations and the anticipated gain in performance is smaller.

Note that there is no attempt to deal with correlations at the channel level. This aspect is implicitly addressed in the OSS multi-channel training. For instance, if two channels are "perfectly" (i.e. within model accuracy) correlated, they will be attributed the same nodes and the time spent performing the computation for the two channels will be half that required for performing the same computation with our original approach. There is little to be gained by training the model on spectra compressed using PCA or other linear radiance transformation. However, if desired, such transformations can be performed in the model (with no penalty on the computational efficiency) by simply modifying the OSS weights.

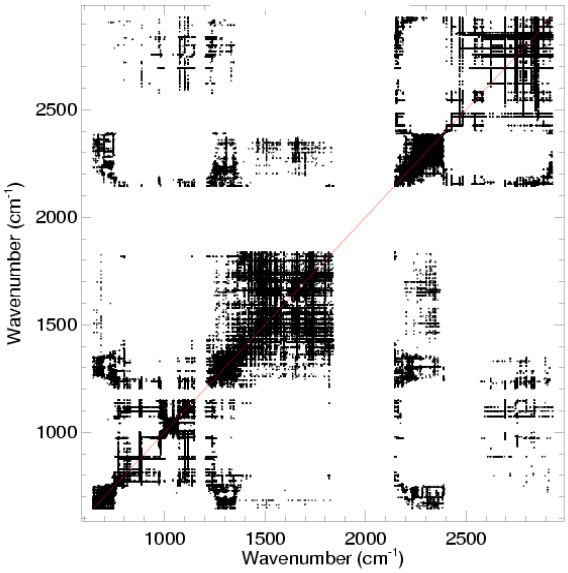

Figure 3: Inter-nodal correlation for the 645-2690 cm^{-1} domain. The figure shows the spectral position of the nodes which are within a correlation radius of 0.01 of any given node in the spectral domain.

Table 1: Average number of selected nodes per channel for 1 cm^{-1} wide boxcars, with single and multi-channel training.

Interval (cm^{-1})	Interval width (cm^{-1})	# nodes (single channel approach)	Gain (multi-channel approach)
645-675	30	286	9
780-820	40	141	6
645-745	100	1047	20
780-880	100	248	10
780-980	200	478	16

3. GENERALIZED CLOUDY TRAINING

The main challenge with the generalized training is coming up with the proper methodology for handling of the slowly varying spectral functions (cloud and/or surface optical properties) across wide intervals. In this case, one cannot simply extend the data set to include a mixture of clear and cloudy scenes and train the model as it is done for clear-sky applications. Because of the large magnitude of their impact on the radiance, clouds tend to drive the selection at the beginning of the process. The presence of clouds tends to smear the spectral features in the TOA radiances and makes the radiance spectra easier to fit, which results in a degraded clear-sky performance. This problem may be partially circumvented by separating clear and cloudy scenes and minimizing the *rms* errors separately for the two sets. However, it is our experience that the solution remains overly sensitive to the range of cloud optical depths used to in the training scenes, an indication that appropriate physical constraints are lacking.

The preferred training approach (used as a benchmark in our future work) follows a two step procedure. In the first step, we apply the generalized clear-sky training described in the previous section. In the second step, the same selection algorithm operates on an initial set of nodes obtained by redistributing the nodes selected in the first step at regular frequency intervals within the specified domain. In this operation, the original wavenumber information associated with each node is lost. The monochromatic radiances at the newly assigned ν_j's (corresponding to the new frequency grid) are used to predict the impact of the slowly varying functions across the entire domain.

The physical basis of the approach is illustrated in Figure 4. In OSS, the same node *i* represents a number of "micro-intervals" (denoted by the index *ik*) with same absorption properties. The OSS weights can be interpreted as the sum of the widths $\Delta\nu_{ik}$ of these micro-intervals divided by the total width of the domain. In the absence of clouds/aerosols, the radiances in the micro-intervals associated with the same index *i* are identical. In the example shown in Figure 4, the contribution of the cloud to the radiance is linear in wavenumber. In this case, the cloudy radiances in the micro-intervals *ik* can be predicted from the radiance values computed at two arbitrarily selected wavenumbers ν_1 and ν_2 within the domain. The expression for the average radiance in any channel within the domain is simply obtained by summing up the contributions of all the micro-intervals for all nodes,

$$\begin{aligned}\bar{R} &= \sum_i w_i \sum_k \frac{\Delta\nu_{ik}}{\Delta\nu_i}\left(a_{ik}R_i(\nu_1)+(1-a_{ik})R_i(\nu_2)\right) \\ &= \sum_i w'_{i1}R_i(\nu_1)+w'_{i2}R_i(\nu_2)\end{aligned} \quad (2)$$

The only difference between Equations (2) and (1) (aside from the fact that some nodes have been duplicated through the cloudy training process) is the introduction in (2) of an extra frequency index for the monochromatic radiance calculations. The selection scheme does not duplicate a node if 1) the molecular absorption is so strong that clouds do not affect the radiances or 2) the impact of spectral variations in cloud properties over the domain spanned by the micro-regions it represents is negligible.

The above method has the advantage that it is robust and stable with respect to the choice of training scenes. It also guarantees by construction that the initial clear-sky solution remains intact. Note that for the selection process to converge, it is important to impose the following constraint on the weights,

$$\sum_j w'_{ij} = w_i \,.$$

The applicability of the method is not limited to the linear case. For more complex functions, some nodes may be tripled, quadrupled…etc, depending on the degree of the polynomial that fits the cloudy radiances over wider intervals.

Figure 5 shows an example of application of the generalized cloudy training to AIRS. Only the first 1262 channels were considered. In this case, cloud/aerosols optical properties were modeled by starting with randomly generated piecewise linear functions (20 cm^{-1} segments) and by fitting a polynomial through the hinge points to smooth the

functions. The loose constraints on the spectral slope and change of slope at the hinge points were derived from realistic cloud/aerosol absorption spectra and correspond to a worst case scenario. This particular training set was designed to accommodate a broad range of ground-based and airborne applications. Note that in Figure 5 there is a tendency for the performance to improve as clouds become more opaque, a desirable property of the approach. For this case, the average number of nodes per channel is 0.82 (0.59 for clear-sky selection) compared 1.98 with the current single channel training, which represents a gain of 2.4 (3.4) in model speed. An AIRS model is currently being trained using more realistic water/ice cloud properties. In this case, higher computational gains may be expected.

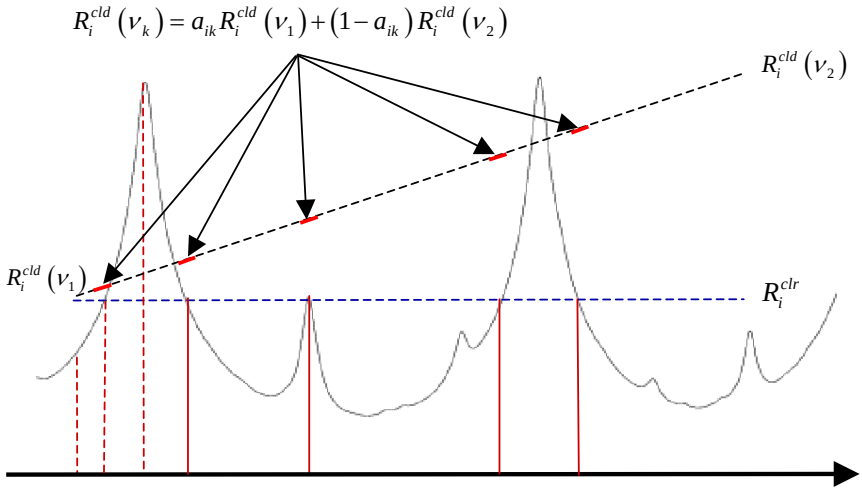

Figure 4: Example of clear-sky (1st step) node selection (dashed lines) for an arbitrary spectral domain encompassing a single broadband channel or multiple high-resolution channels. The 4 other spectral sub-intervals represented by the node *i*=2 are indicated by the solid vertical lines. Clear sky radiances are the same in all the 5 sub-intervals. The impact of clouds on the radiances for this node (linear case) is indicated by the upper dashed line.

4. OSS VALIDATION IN SCATTERING ATMOSPHERES

The OSS method is by construction amenable to the treatment of radiative transfer in scattering atmospheres. However, one has yet to devise an approach for performing the training in such conditions. There are two aspects of this problem that must be considered separately. The first question is how one should train the OSS model for a single narrow channel, when cloud/aerosol optical properties do not vary spectrally within the channel, and the second issue relates to the handling of the spectral variations of cloud properties across a wide band channel (or, for generalized training – see previous section, across multiple channels). The first question is addressed in this section. Our effort has initially focused on the thermal regime.

The effect of introducing scatterers is to increase the photons path lengths within the atmospheric layers below the cloud top. As long as cloud properties do not vary across the channel, there is *a priori* no need to use a scattering model in order to perform the training. Clear scenes constructed by using a wide enough range of path lengths within appropriately selected layers should be adequate.

The first step has been to validate an OSS model trained with our current clear-sky training data set (without any perturbation in the layer air masses) over the full range of cloud/aerosol optical depths and single scatter albedos. The particular model used in this study was trained for 1 cm^{-1} boxcar functions with a nominal accuracy of 0.05 K. The reference calculations were produced using LBLRTM (Clough *et al.*, 1992) combined with the CHARTS (Moncet and Clough, 1997) adding-doubling RT model. Figure 1 shows examples of errors obtained with low and high single layer clouds. It is apparent from this figure that the current model behaves very well in the thermal regime. For single scatter albedos up to 0.95, the cloudy performance is similar to the clear-sky performance and radiance errors are within the tolerance of the model. There is a sudden increase in the error when the cloud single scatter albedos approaches 1, which becomes apparent only at high optical depths (50 or greater). Even in this case, the error relative to line-by-line calculations is within ~0.2K. These preliminary results are quite encouraging. Some ongoing effort is aimed at improving the performance in highly reflective situations and modifying the training to accommodate the solar regime.

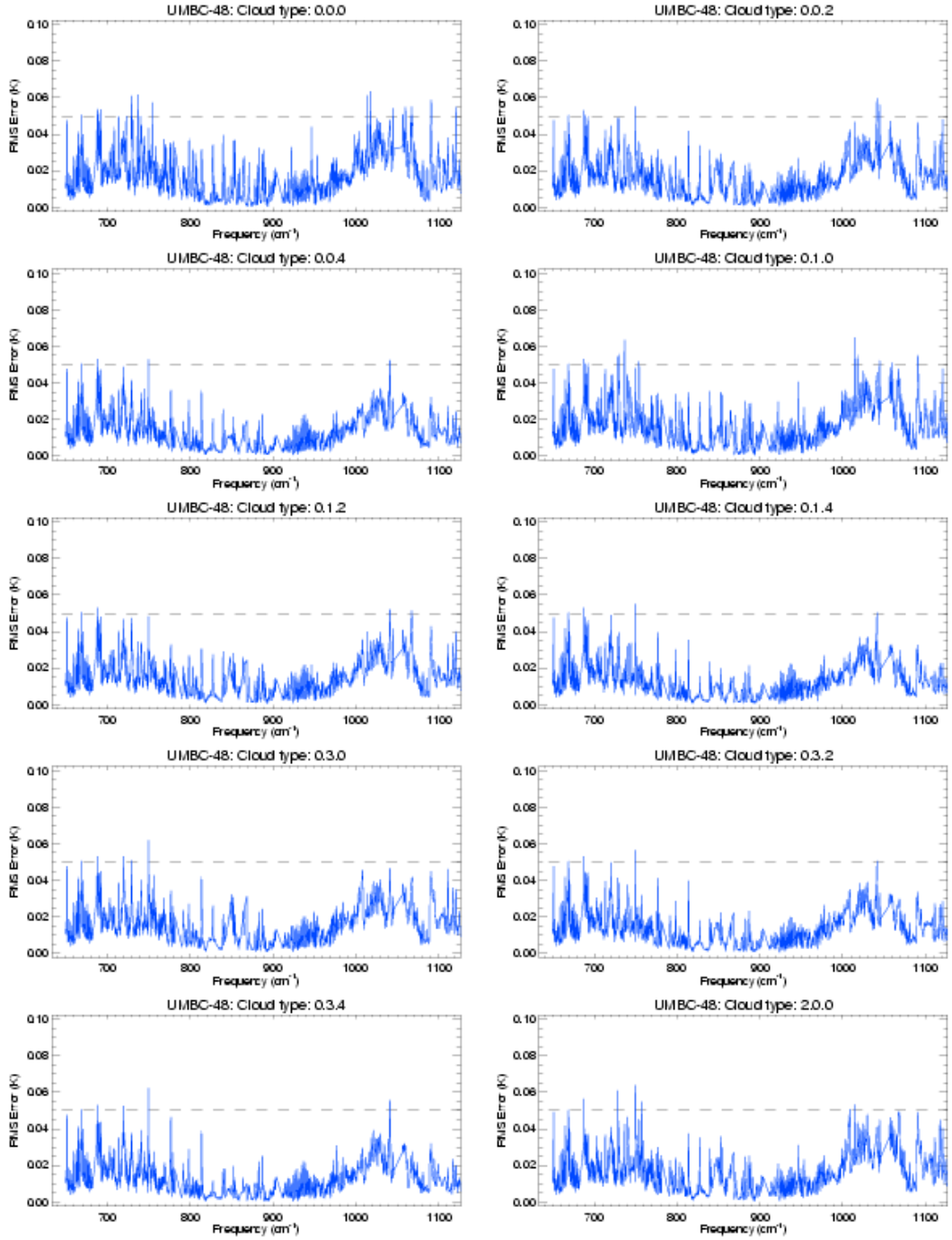

Figure 5: OSS model accuracy in multi-layer cloudy (purely absorbing case) atmospheres. The upper left plot represent the rms errors in the clear-sky based on 48 profiles from the UMBC standard data set. The remaining plots correspond to different ranges of cloud optical depth in 3 atmospheric layers (low, medium, high). The range of optical depth (OD) corresponding to each layer is indicated by the 3 indices at the top of each plot, the lower layer being represented by the 1st index. The code used is: 0 = clear, 1= OD < 0.5, 2= OD <1, 3= OD < 2, and 4= OD > 2.

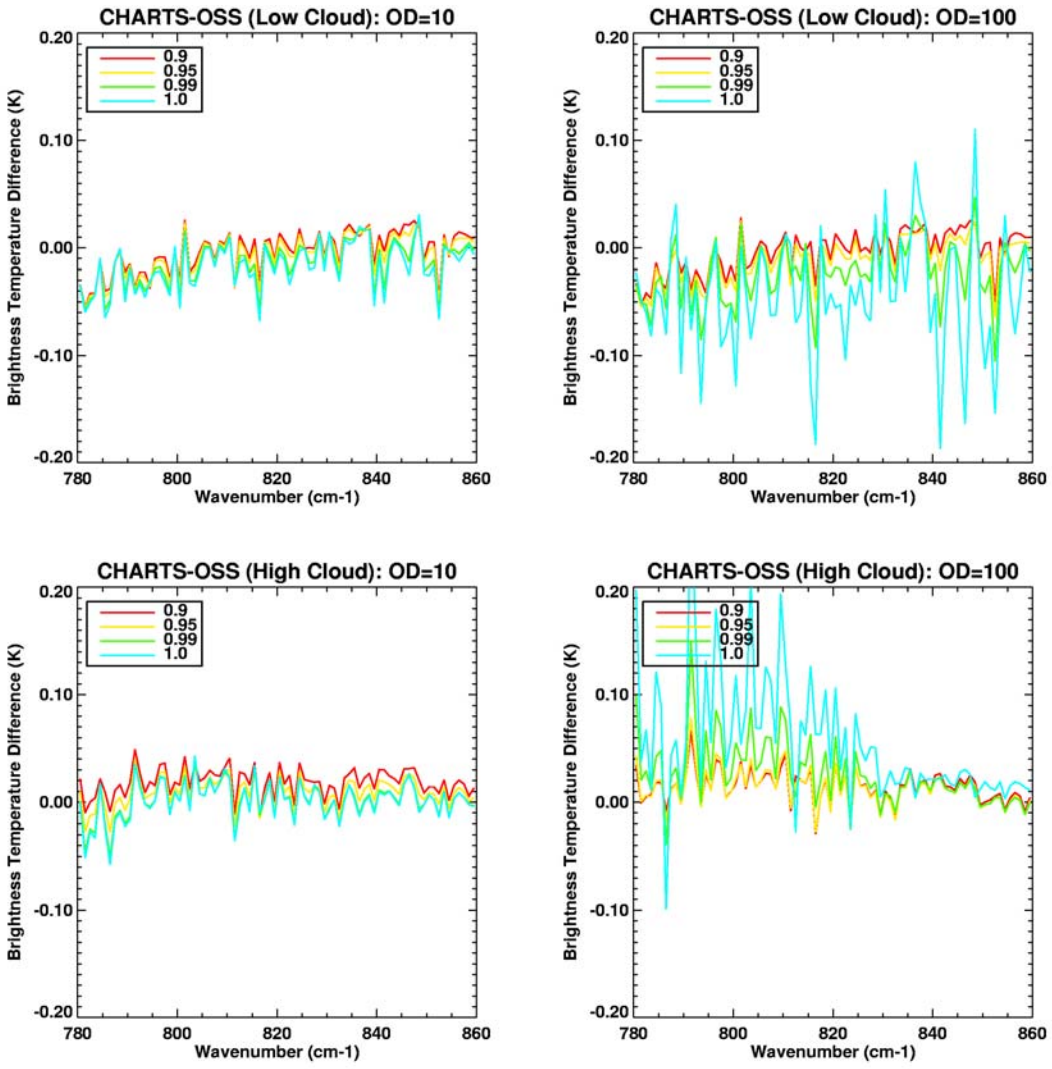

Figure 6: OSS modeling errors for UMBC profile #1 (Nadir viewing) with low (top pressure = 800mb) and high (top pressure = 150mb) clouds. The results shown in this figure correspond to cloud optical depths of 10 (left) and 100 (right) and single scatter albedos ranging from 0.9 to 1. Clear-sky training was used.

5. SUMMARY

The current development of OSS addresses applications to scattering atmospheres and generalized multi-channel training. We have shown that models produced with the current clear-sky training should provide satisfactory results in cloudy skies in the thermal regime (both microwave and infrared). Until the cloudy training is refined, some caution should be exercised when using those models in highly reflective clouds and at large viewing angles. A second important development is the generalization of the training to multiple channels. Speed gains over the current approach of up to 10-20 (depending on the instrument) may be anticipated when training OSS to simultaneously fit radiances/transmittances over the entire set or a subset of high resolution channels. The effect of clouds/aerosols is to reduce the large scale correlations. For cloudy radiances the minimum gain (i.e. worst case) is around 2-3 for AIRS. As part of this effort we also introduced a new approach for handling spectral variations in cloud/surface optical properties in the training. This approach clearly distinguishes between the application of the OSS formalism for modeling the gaseous transmittance and its extension to radiance modeling for capturing the slowly varying spectral functions across wide spectral domains. The robustness of the training is key requirement for providing unsupervised training capabilities and for minimizing model validation work. Future work includes refining the OSS training in scattering atmospheres, both in the thermal and solar regimes, and improving the generalized multi-channel training. A first stable version of an AIRS model trained with this latter scheme should be available in the fall of 2005.

6. REFERENCES

Armbruster, W. and J. Fischer, 1996: Improved method of exponential sum fitting of transmissions to describe the absorption of atmospheric gases, *Applied Optics*, 35, pp.1931-1941

Atmospheric and Environmental Research, Inc., 2004, "Algorithm Theoretical Basis Document for the Cross-Track Infrared Sounder (CrIS): Volume 2: Environmental Data Records", Version 4.0.

Atmospheric and Environmental Research, Inc., 2001, "Algorithm Theoretical Basis Document for the Conical-Scanning Microwave Imager/Sounder (CMIS) Environmental Data Records (EDRs), Volume 2: Core Physical Inversion Module", Version 1.4.

Atmospheric and Environmental Research, Inc., 2002, "Algorithm Theoretical Basis Document for the Infrared Total Column Ozone Algorithm for the Ozone Mapping and Profiler Suite (OMPS)", Version 5.0.

Clough, S.A., Iacono, M.J. and Moncet, J.-L., 1992, "Line-by-line calculation of atmospheric fluxes and cooling rates: Application to water vapor", *J. Geophys. Res.*, **97**, pp. 15761-785.

Goody, R., West, R., Chen, L. and Crisp, D., 1989: The correlated-k method for radiation calculations in nonhomogeneous atmospheres, *J. Quant. Spectr. Rad. Tran.*, **42**, pp.539-550

Moncet, J.-L., Uymin, G. and Snell, H.E., 2004, "Atmospheric radiance modeling using the Optimal Spectral Sampling (OSS) method", *SPIE* 5425-37.

Moncet, J.-L. and Uymin, G., 2003, "Infrared radiative transfer modeling using the Optimal Spectral Sampling (OSS) method", paper 4.6 presented at ITSC XIII, Sainte Adele, Canada.

Moncet, J.-L. and Uymin, G., 2003, "Infrared radiative transfer modeling using the Optimal Spectral Sampling (OSS) method", poster B20 presented at ITSC XIII, Sainte Adele, Canada.

Moncet, J.-L. and Clough, S.A., 1997, "Accelerated monochromatic radiative transfer for scattering atmospheres: Application of a new model to spectral radiance observations", *J. Geophys. Res.*, **102**, 21,853-866.

van Delst, P., Han, Y. and Liu, Q., 2005, "JCSDA Community Radiative Transfer Model (CRTM)", 5th MURI Workshop, Madison WI

Weng, F. *et al*., 2005, "Development of the JCSDA Community Radiative Transfer Model (CRTM)", presented at ITSC XIV, Beijing, China.

Wiscombe, W. J. and J. W. Evans, 1977: Exponential-sum fitting of radiative transmission functions, *J. of Comp. Phys.*, **24**, pp.416-444